

Relativistic effects in the galaxy number counts bispectrum as a new tool in cosmology

Giovanni Marozzi

Instituto de Cosmologia, Relatividade e Astrofísica
Centro Brasileiro de Pesquisas Físicas



2nd FLAG meeting
The Quantum and Gravity,
University of Trento
08 June 2016

Outline

- Introduction
- Geodesic light-cone (GLC) coordinates and cosmological observables
- From GLC to the Poisson gauge: describing the middle non-linear regime
- Galaxy Number Counts: impact of the magnification bias to second order
- Galaxy Number Counts bispectrum
- Conclusions

Mainly based on:

M. Gasperini, GM, F. Nugier, G. Veneziano, JCAP 07 (2011) 008;
G. Fanizza, M. Gasperini, GM, G. Veneziano, JCAP 11 (2013) 019;
E. Di Dio, R. Durrer, GM, F. Montanari, JCAP 12 (2014) 017;
E. Di Dio, R. Durrer, GM, F. Montanari, JCAP 01 (2016) 016.

Outline

- Introduction
- Geodesic light-cone (GLC) coordinates and cosmological observables
- From GLC to the Poisson gauge: describing the middle non-linear regime
- Galaxy Number Counts: impact of the magnification bias to second order
- Galaxy Number Counts bispectrum
- Conclusions

Mainly based on:

M. Gasperini, GM, F. Nugier, G. Veneziano, JCAP 07 (2011) 008;
G. Fanizza, M. Gasperini, GM, G. Veneziano, JCAP 11 (2013) 019;
E. Di Dio, R. Durrer, GM, F. Montanari, JCAP 12 (2014) 017;
E. Di Dio, R. Durrer, GM, F. Montanari, JCAP 01 (2016) 016.

Outline

- Introduction
- Geodesic light-cone (GLC) coordinates and cosmological observables
- From GLC to the Poisson gauge: describing the middle non-linear regime
- Galaxy Number Counts: impact of the magnification bias to second order
- Galaxy Number Counts bispectrum
- Conclusions

Mainly based on:

M. Gasperini, GM, F. Nugier, G. Veneziano, JCAP 07 (2011) 008;
G. Fanizza, M. Gasperini, GM, G. Veneziano, JCAP 11 (2013) 019;
E. Di Dio, R. Durrer, GM, F. Montanari, JCAP 12 (2014) 017;
E. Di Dio, R. Durrer, GM, F. Montanari, JCAP 01 (2016) 016.

Outline

- Introduction
- Geodesic light-cone (GLC) coordinates and cosmological observables
- From GLC to the Poisson gauge: describing the middle non-linear regime
- Galaxy Number Counts: impact of the magnification bias to second order
- Galaxy Number Counts bispectrum
- Conclusions

Mainly based on:

M. Gasperini, GM, F. Nugier, G. Veneziano, JCAP 07 (2011) 008;
G. Fanizza, M. Gasperini, GM, G. Veneziano, JCAP 11 (2013) 019;
E. Di Dio, R. Durrer, GM, F. Montanari, JCAP 12 (2014) 017;
E. Di Dio, R. Durrer, GM, F. Montanari, JCAP 01 (2016) 016.

Outline

- Introduction
- Geodesic light-cone (GLC) coordinates and cosmological observables
- From GLC to the Poisson gauge: describing the middle non-linear regime
- Galaxy Number Counts: impact of the magnification bias to second order
- Galaxy Number Counts bispectrum
- Conclusions

Mainly based on:

M. Gasperini, GM, F. Nugier, G. Veneziano, JCAP 07 (2011) 008;
G. Fanizza, M. Gasperini, GM, G. Veneziano, JCAP 11 (2013) 019;
E. Di Dio, R. Durrer, GM, F. Montanari, JCAP 12 (2014) 017;
E. Di Dio, R. Durrer, GM, F. Montanari, JCAP 01 (2016) 016.

Outline

- Introduction
- Geodesic light-cone (GLC) coordinates and cosmological observables
- From GLC to the Poisson gauge: describing the middle non-linear regime
- Galaxy Number Counts: impact of the magnification bias to second order
- Galaxy Number Counts bispectrum
- Conclusions

Mainly based on:

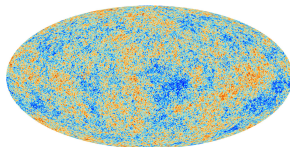
M. Gasperini, GM, F. Nugier, G. Veneziano, JCAP 07 (2011) 008;
G. Fanizza, M. Gasperini, GM, G. Veneziano, JCAP 11 (2013) 019;
E. Di Dio, R. Durrer, GM, F. Montanari, JCAP 12 (2014) 017;
E. Di Dio, R. Durrer, GM, F. Montanari, JCAP 01 (2016) 016.

The Problem

Cosmology has entered a precision era.

The present and future main sources of data are:

- CMB anisotropies
(2 dimensional dataset).

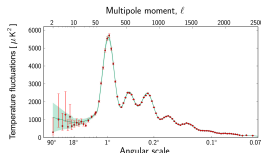


CMB sky as seen by Planck

Link between data and models made mostly using linear perturbation theory.

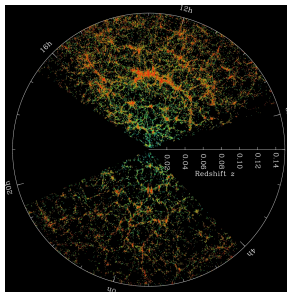
$$D_l = l(l+1)C_l/(2\pi)$$

Planck Collaboration: Planck 2013 results XV
CMB power spectra and likelihood



The Problem

- Large scale structure observations (3 dimensional dataset).



Sloan Digital Sky Team

For LSS, on intermediate to small scales, non-linearities become important.



Much more information, but analysis more complicated.

We need not only accurate observations, but also an accurate model!

What are LSS surveys really observing?

- All observations are made over the past light-cone with redshift and incoming photons direction as observable coordinates.
- The measured redshift is perturbed by peculiar velocities and by the gravitational potential.
- The observed volume is distorted.
- The angles we are looking into are not the ones which identify the source/galaxy from which the photons have been emitted.
- For small galaxy catalogs these effects are not very important, but when we go out to $z \sim 1$ or more they become relevant. Already for SDSS ($z \sim 0.2$ for the main catalog) or, even more, BOSS ($z \sim 0.6$) they should be taken in account.
- But of course much more for surveys like DES, bigBOSS and EUCLID.

What are LSS surveys really observing?

- All observations are made over the past light-cone with redshift and incoming photons direction as observable coordinates.
- The measured redshift is perturbed by peculiar velocities and by the gravitational potential.
- The observed volume is distorted.
- The angles we are looking into are not the ones which identify the source/galaxy from which the photons have been emitted.
- For small galaxy catalogs these effects are not very important, but when we go out to $z \sim 1$ or more they become relevant. Already for SDSS ($z \sim 0.2$ for the main catalog) or, even more, BOSS ($z \sim 0.6$) they should be taken in account.
- But of course much more for surveys like DES, bigBOSS and EUCLID.

What are LSS surveys really observing?

- All observations are made over the past light-cone with redshift and incoming photons direction as observable coordinates.
- The measured redshift is perturbed by peculiar velocities and by the gravitational potential.
- The observed volume is distorted.
- The angles we are looking into are not the ones which identify the source/galaxy from which the photons have been emitted.
- For small galaxy catalogs these effects are not very important, but when we go out to $z \sim 1$ or more they become relevant. Already for SDSS ($z \sim 0.2$ for the main catalog) or, even more, BOSS ($z \sim 0.6$) they should be taken in account.
- But of course much more for surveys like DES, bigBOSS and EUCLID.

What are LSS surveys really observing?

- All observations are made over the past light-cone with redshift and incoming photons direction as observable coordinates.
- The measured redshift is perturbed by peculiar velocities and by the gravitational potential.
- The observed volume is distorted.
- The angles we are looking into are not the ones which identify the source/galaxy from which the photons have been emitted.
- For small galaxy catalogs these effects are not very important, but when we go out to $z \sim 1$ or more they become relevant. Already for SDSS ($z \sim 0.2$ for the main catalog) or, even more, BOSS ($z \sim 0.6$) they should be taken in account.
- But of course much more for surveys like DES, bigBOSS and EUCLID.

What are LSS surveys really observing?

- All observations are made over the past light-cone with redshift and incoming photons direction as observable coordinates.
- The measured redshift is perturbed by peculiar velocities and by the gravitational potential.
- The observed volume is distorted.
- The angles we are looking into are not the ones which identify the source/galaxy from which the photons have been emitted.
- For small galaxy catalogs these effects are not very important, but when we go out to $z \sim 1$ or more they become relevant. Already for SDSS ($z \sim 0.2$ for the main catalog) or, even more, BOSS ($z \sim 0.6$) they should be taken in account.
- But of course much more for surveys like DES, bigBOSS and EUCLID.

What are LSS surveys really observing?

- All observations are made over the past light-cone with redshift and incoming photons direction as observable coordinates.
- The measured redshift is perturbed by peculiar velocities and by the gravitational potential.
- The observed volume is distorted.
- The angles we are looking into are not the ones which identify the source/galaxy from which the photons have been emitted.
- For small galaxy catalogs these effects are not very important, but when we go out to $z \sim 1$ or more they become relevant. Already for SDSS ($z \sim 0.2$ for the main catalog) or, even more, BOSS ($z \sim 0.6$) they should be taken in account.
- But of course much more for surveys like DES, bigBOSS and EUCLID.

Observing the large scale structure of the Universe: k -space vs ℓ -space

- Summarizing: both our observable coordinates and the observed volume are distorted by the presence of inhomogeneities.
- **Standard Newtonian effects.** Usually described in k -space, where the result depends not only on the observations but also on the cosmological model assumed which relates redshifts and angles to distances.
- **Relativistic effects.** Among which lensing effects involve integrals over the past light-cone and have a translation in k -space not straightforward.
- A maybe better choice: report results from perturbation theory in ℓ -space and redshift space, so that they can be directly compared with observations without any assumptions on the cosmology.

For 2-point correlation functions \Rightarrow We have to go beyond Newtonian gravity!

For 3-point correlation functions \Rightarrow We have to go beyond Newtonian gravity and beyond linear theory!

Observing the large scale structure of the Universe: k -space vs ℓ -space

- Summarizing: both our observable coordinates and the observed volume are distorted by the presence of inhomogeneities.
- **Standard Newtonian effects.** Usually described in k -space, where the result depends not only on the observations but also on the cosmological model assumed which relates redshifts and angles to distances.
- **Relativistic effects.** Among which lensing effects involve integrals over the past light-cone and have a translation in k -space not straightforward.
- A maybe better choice: report results from perturbation theory in ℓ -space and redshift space, so that they can be directly compared with observations without any assumptions on the cosmology.

For 2-point correlation functions \Rightarrow We have to go beyond Newtonian gravity!

For 3-point correlation functions \Rightarrow We have to go beyond Newtonian gravity and beyond linear theory!

Observing the large scale structure of the Universe:

k -space vs ℓ -space

- Summarizing: both our observable coordinates and the observed volume are distorted by the presence of inhomogeneities.
- **Standard Newtonian effects.** Usually described in k -space, where the result depends not only on the observations but also on the cosmological model assumed which relates redshifts and angles to distances.
- **Relativistic effects.** Among which lensing effects involve integrals over the past light-cone and have a translation in k -space not straightforward.
- A maybe better choice: report results from perturbation theory in ℓ -space and redshift space, so that they can be directly compared with observations without any assumptions on the cosmology.

For 2-point correlation functions \Rightarrow We have to go beyond Newtonian gravity!

For 3-point correlation functions \Rightarrow We have to go beyond Newtonian gravity and beyond linear theory!

Observing the large scale structure of the Universe:

k -space vs ℓ -space

- Summarizing: both our observable coordinates and the observed volume are distorted by the presence of inhomogeneities.
- **Standard Newtonian effects.** Usually described in k -space, where the result depends not only on the observations but also on the cosmological model assumed which relates redshifts and angles to distances.
- **Relativistic effects.** Among which lensing effects involve integrals over the past light-cone and have a translation in k -space not straightforward.
- A maybe better choice: report results from perturbation theory in ℓ -space and redshift space, so that they can be directly compared with observations without any assumptions on the cosmology.

For 2-point correlation functions \Rightarrow We have to go beyond Newtonian gravity!

For 3-point correlation functions \Rightarrow We have to go beyond Newtonian gravity and beyond linear theory!

Observing the large scale structure of the Universe: k -space vs ℓ -space

- Summarizing: both our observable coordinates and the observed volume are distorted by the presence of inhomogeneities.
- **Standard Newtonian effects.** Usually described in k -space, where the result depends not only on the observations but also on the cosmological model assumed which relates redshifts and angles to distances.
- **Relativistic effects.** Among which lensing effects involve integrals over the past light-cone and have a translation in k -space not straightforward.
- A maybe better choice: report results from perturbation theory in ℓ -space and redshift space, so that they can be directly compared with observations without any assumptions on the cosmology.

For 2-point correlation functions \Rightarrow We have to go beyond Newtonian gravity!

For 3-point correlation functions \Rightarrow We have to go beyond Newtonian gravity and beyond linear theory!

Outline

- Introduction
- Geodesic light-cone (GLC) coordinates and cosmological observables
- From GLC to the Poisson gauge: describing the middle non-linear regime
- Galaxy Number Counts: impact of the magnification bias to second order
- Galaxy Number Counts bispectrum
- Conclusions

Geodesic light-cone coordinates

An adapted light-cone coordinate system $x^\mu = (w, \tau, \tilde{\theta}^a)$, $a = 1, 2$ can be defined by the following metric (Gasperini, GM, Nugier, Veneziano (2011)):

$$ds^2 = \Upsilon^2 dw^2 - 2\Upsilon dw d\tau + \gamma_{ab}(d\tilde{\theta}^a - U^a dw)(d\tilde{\theta}^b - U^b dw); \quad a, b = 1, 2,$$

which depends on six arbitrary functions: Υ , the two-dimensional vector U^a and the symmetric tensor γ_{ab} .

w is a null coordinate, $\partial_\mu \tau$ defines a geodesic flow

$k^\mu = g^{\mu\nu} \partial_\nu w = g^{\mu w} = -\delta_\tau^\mu \Upsilon^{-1}$ null geodesics connecting sources and observer



Photons travel at constant w and $\tilde{\theta}^a$

Spatially flat FLRW limit

$$w = r + \eta, \quad \tau = t, \quad \Upsilon = a(t), \quad U^a = 0, \\ \gamma_{ab} d\tilde{\theta}^a d\tilde{\theta}^b = a^2(t) r^2 (d\theta^2 + \sin^2 \theta d\phi^2),$$

where η is the conformal time of the homogeneous metric: $d\eta = dt/a$.

Geodesic light-cone coordinates

An adapted light-cone coordinate system $x^\mu = (w, \tau, \tilde{\theta}^a)$, $a = 1, 2$ can be defined by the following metric (Gasperini, GM, Nugier, Veneziano (2011)):

$$ds^2 = \Upsilon^2 dw^2 - 2\Upsilon dw d\tau + \gamma_{ab}(d\tilde{\theta}^a - U^a dw)(d\tilde{\theta}^b - U^b dw); \quad a, b = 1, 2,$$

which depends on six arbitrary functions: Υ , the two-dimensional vector U^a and the symmetric tensor γ_{ab} .

w is a null coordinate, $\partial_\mu \tau$ defines a geodesic flow

$k^\mu = g^{\mu\nu} \partial_\nu w = g^{\mu w} = -\delta_\tau^\mu \Upsilon^{-1}$ null geodesics connecting sources and observer



Photons travel at constant w and $\tilde{\theta}^a$

Spatially flat FLRW limit

$$\begin{aligned} w &= r + \eta, & \tau &= t, & \Upsilon &= a(t), & U^a &= 0, \\ \gamma_{ab} d\tilde{\theta}^a d\tilde{\theta}^b &= a^2(t) r^2 (d\theta^2 + \sin^2 \theta d\phi^2), \end{aligned}$$

where η is the conformal time of the homogeneous metric: $d\eta = dt/a$.

Red shift and Area Distance

The exact non-perturbative redshift is given by

$$1 + z_s = \frac{(k^\mu u_\mu)_s}{(k^\mu u_\mu)_o} = \frac{(\partial^\mu w \partial_\mu \tau)_s}{(\partial^\mu w \partial_\mu \tau)_o} = \frac{\Upsilon(w_o, \tau_o, \tilde{\theta}^a)}{\Upsilon(w_o, \tau_s, \tilde{\theta}^a)}$$

where the subscripts “o” and “s” denote, respectively, a quantity evaluated at the observer and source space-time position.

The area distance d_A , related to the luminosity distance d_L of a source at redshift z_s by the Etherington (or reciprocity) relation

$$d_A = (1 + z_s)^{-2} d_L ,$$

is given by

$$d_A^2 \equiv \frac{dS}{d\Omega_o} ,$$

where $d\Omega_o$ is the infinitesimal solid angle at the observer, and dS is the cross-sectional area element perpendicular to the light ray at the source.

Galaxy Number Counts

Galaxy Number Counts= number N of sources (galaxies) per solid angle and redshift.

The fluctuation of the galaxy number counts in function of observed redshift and direction is defined by

$$\Delta(\mathbf{n}, z) \equiv \frac{N(\mathbf{n}, z) - \langle N \rangle(z)}{\langle N \rangle(z)},$$

where

$$N(\mathbf{n}, z) = \rho(\mathbf{n}, z) V(\mathbf{n}, z).$$

Considering the density and volume fluctuations per redshift bin dz and per solid angle $d\Omega$

$$V(\mathbf{n}, z) = \bar{V}(z) \left(1 + \frac{\delta V^{(1)}}{\bar{V}} + \frac{\delta V^{(2)}}{\bar{V}} \right)$$

$$\rho(\mathbf{n}, z) = \bar{\rho}(z) \left(1 + \delta^{(1)} + \delta^{(2)} \right),$$

we can give the directly observed number fluctuations

$$\Delta(\mathbf{n}, z) = \left[\delta^{(1)} + \frac{\delta V^{(1)}}{\bar{V}} + \delta^{(1)} \frac{\delta V^{(1)}}{\bar{V}} + \delta^{(2)} + \frac{\delta V^{(2)}}{\bar{V}} - \left\langle \delta^{(1)} \frac{\delta V^{(1)}}{\bar{V}} \right\rangle - \langle \delta^{(2)} \rangle - \left\langle \frac{\delta V^{(2)}}{\bar{V}} \right\rangle \right]$$

Volume Perturbation

The 3-dimensional volume element dV seen by a source with 4-velocity u^μ is

$$dV = \sqrt{-g} \epsilon_{\mu\nu\alpha\beta} u^\mu dx^\nu dx^\alpha dx^\beta .$$

In terms of the observed quantities (z, θ_o, ϕ_o)

$$dV = \sqrt{-g} \epsilon_{\mu\nu\alpha\beta} u^\mu \frac{\partial x^\nu}{\partial z} \frac{\partial x^\alpha}{\partial \theta_s} \frac{\partial x^\beta}{\partial \phi_s} \left| \frac{\partial (\theta_s, \phi_s)}{\partial (\theta_o \phi_o)} \right| dz d\theta_o d\phi_o \equiv v(z, \theta_o, \phi_o) dz d\theta_o d\phi_o .$$

Going to GLC we then have

$$dV = -\sqrt{-g} u^w \frac{\partial \tau}{\partial z} dz d\theta_o d\phi_o .$$

and

$$dV = \sqrt{|\gamma|} \left(-\frac{d\tau}{dz} \right) dz d\theta_o d\phi_o , \quad \text{or} \quad v = \sqrt{|\gamma|} \left(-\frac{d\tau}{dz} \right)$$

This is a non-perturbative expression for the volume element at the source in terms of the observed redshift and the observation angles in GLC gauge.

If we would know $\rho(\mathbf{n}, z)$ non-perturbatively we could write the number counts in an exact way in GLC.

Volume Perturbation

The 3-dimensional volume element dV seen by a source with 4-velocity u^μ is

$$dV = \sqrt{-g} \epsilon_{\mu\nu\alpha\beta} u^\mu dx^\nu dx^\alpha dx^\beta.$$

In terms of the observed quantities (z, θ_o, ϕ_o)

$$dV = \sqrt{-g} \epsilon_{\mu\nu\alpha\beta} u^\mu \frac{\partial x^\nu}{\partial z} \frac{\partial x^\alpha}{\partial \theta_s} \frac{\partial x^\beta}{\partial \phi_s} \left| \frac{\partial (\theta_s, \phi_s)}{\partial (\theta_o \phi_o)} \right| dz d\theta_o d\phi_o \equiv v(z, \theta_o, \phi_o) dz d\theta_o d\phi_o.$$

Going to GLC we then have

$$dV = -\sqrt{-g} u^w \frac{\partial \tau}{\partial z} dz d\theta_o d\phi_o.$$

and

$$dV = \sqrt{|\gamma|} \left(-\frac{d\tau}{dz} \right) dz d\theta_o d\phi_o, \quad \text{or} \quad v = \sqrt{|\gamma|} \left(-\frac{d\tau}{dz} \right)$$

This is a non-perturbative expression for the volume element at the source in terms of the observed redshift and the observation angles in GLC gauge.

If we would know $\rho(\mathbf{n}, z)$ non-perturbatively we could write the number counts in an exact way in GLC.

Outline

- Introduction
- Geodesic light-cone (GLC) coordinates and cosmological observables
- From GLC to the Poisson gauge: describing the middle non-linear regime
- Galaxy Number Counts: impact of the magnification bias to second order
- Galaxy Number Counts bispectrum
- Conclusions

Coordinates Transformation

Let us consider a stochastic background of scalar perturbations on a conformally flat FLRW space-time to describe the inhomogeneities of our Universe at large scale.

Using spherical coordinates ($y^\mu = (\eta, r, \theta, \phi)$) in the Poisson gauge (PG) we have

$$g_{NG}^{\mu\nu} = a^{-2}(\eta) \text{diag} \left(-1 + 2\Phi, 1 + 2\Psi, (1 + 2\Psi)\gamma_0^{ab} \right)$$

where $\gamma_0^{ab} = \text{diag} \left(r^{-2}, r^{-2} \sin^{-2} \theta \right)$, $\Phi = \Psi^{(1)} + \Phi^{(2)} - 2(\Psi^{(1)})^2$ and $\Psi = \Psi^{(1)} + \Psi^{(2)} + 2(\Psi^{(1)})^2$.

To use the previous results we have to re-express this metric in GLC form. We define the coordinates transformation using

$$g_{GLC}^{\rho\sigma}(x) = \frac{\partial x^\rho}{\partial y^\mu} \frac{\partial x^\sigma}{\partial y^\nu} g_{NG}^{\mu\nu}(y)$$

and imposing the following boundary conditions

- Non-singular transformation around the observer position at $r = 0$.
- The two-dimensional spatial section $r = \text{const}$ is locally parametrized at the observer position by standard spherical coordinates.

Cosmological Observables: redshift

The redshift up to second order in perturbation theory is

$$1 + z = \frac{a(\eta_0)}{a(\eta_s)} \left[1 + \delta^{(1)} z + \delta^{(2)} z \right]$$

with

$$\begin{aligned} \delta z^{(1)} &= -\partial_r v_s^{(1)} - \psi_s^{(1)} - 2 \int_{\eta_s}^{\eta_0} d\eta' \partial_{\eta'} \psi^{(1)}(\eta') \\ \delta z^{(2)} &= -\partial_r v_s^{(2)} - \psi_s^{(2)} - \int_{\eta_s}^{\eta_0} d\eta' \partial_{\eta'} \left[\Phi^{(2)} + \Psi^{(2)} \right](\eta') + \frac{1}{2} (\partial_r v_s)^2 + \frac{1}{2} (\psi_s)^2 \\ &+ (-v_{||s} - \psi_s) \left(-\psi_s - 2 \int_{\eta_s}^{\eta_0} d\eta' \partial_{\eta'} \psi(\eta') \right) + \frac{1}{2} \partial^a v_s \partial_a v_s + 2a \partial^a v_s \partial_a \int_{\eta_s}^{\eta_0} d\eta' \psi(\eta') \\ &+ 4 \int_{\eta_s}^{\eta_0} d\eta' \left[\psi(\eta') \partial_{\eta'} \psi(\eta') + \partial_{\eta'} \psi(\eta') \int_{\eta'}^{\eta_0} d\eta'' \partial_{\eta''} \psi(\eta'') \right. \\ &+ \psi(\eta') \int_{\eta'}^{\eta_0} d\eta'' \partial_{\eta''}^2 \psi(\eta'') - \gamma_0^{ab} \partial_a \left(\int_{\eta'}^{\eta_0} d\eta'' \psi(\eta'') \right) \partial_b \left(\int_{\eta'}^{\eta_0} d\eta'' \partial_{\eta''} \psi(\eta'') \right) \Big] \\ &+ 2\partial_a (\partial_r v_s + \psi_s) \int_{\eta_s}^{\eta_0} d\eta' \gamma_0^{ab} \partial_b \int_{\eta'}^{\eta_0} d\eta'' \psi(\eta'') \\ &+ 4 \int_{\eta_s}^{\eta_0} d\eta' \partial_a \left(\partial_{\eta'} \psi(\eta') \right) \int_{\eta'}^{\eta_0} d\eta'' \gamma_0^{ab} \partial_b \int_{\eta''}^{\eta_0} d\eta''' \psi(\eta''') \end{aligned}$$

Cosmological Observables

To obtain Δ in the PG, in function of the observed redshift and of the direction of observation (θ_o, φ_o) , we have:

Step 1 → Expand the exact expression of Δ in function of the PG coordinate using the coordinate transformation.

Step 2 → Expand conformal time and radial PG coordinates around a fiducial model as $\eta_s = \eta_s^{(0)} + \eta_s^{(1)} + \eta_s^{(2)}$ and $r_s = r_s^{(0)} + r_s^{(1)} + r_s^{(2)}$ perturbatively solving

$$1+z_s = \frac{a(\eta_o)}{a(\eta_s^{(0)})} = \frac{a(\eta_o)}{a(\eta_s)} \left[1 + \delta^{(1)} z + \delta^{(2)} z \right] \quad , \quad w_o = \eta_s^{(0)} + r_s^{(0)} = w^{(0)} + w^{(1)} + w^{(2)}$$

Step 3 → Taylor expand the solution of Step 1 around the fiducial model using Step 2, and around the direction of observation using the fact that $\tilde{\theta}^a = \theta_o^a$ are constant along the line-of-sight and therefore

$$\theta^a = \theta^{a(0)} + \theta^{a(1)} = \theta_o^a - 2 \int_{\eta_s^{(0)}}^{\eta_o} d\eta' \gamma_0^{ab} \partial_b \int_{\eta'}^{\eta_o} d\eta'' \Psi^{(1)}(\eta'', \eta_o - \eta'', \theta_o^a) .$$

Cosmological Observables

To obtain Δ in the PG, in function of the observed redshift and of the direction of observation (θ_o, φ_o) , we have:

Step 1 → Expand the exact expression of Δ in function of the PG coordinate using the coordinate transformation.

Step 2 → Expand conformal time and radial PG coordinates around a fiducial model as $\eta_s = \eta_s^{(0)} + \eta_s^{(1)} + \eta_s^{(2)}$ and $r_s = r_s^{(0)} + r_s^{(1)} + r_s^{(2)}$ perturbatively solving

$$1+z_s = \frac{a(\eta_o)}{a(\eta_s^{(0)})} = \frac{a(\eta_o)}{a(\eta_s)} \left[1 + \delta^{(1)} z + \delta^{(2)} z \right] \quad , \quad w_o = \eta_s^{(0)} + r_s^{(0)} = w^{(0)} + w^{(1)} + w^{(2)}$$

Step 3 → Taylor expand the solution of Step 1 around the fiducial model using Step 2, and around the direction of observation using the fact that $\tilde{\theta}^a = \theta_o^a$ are constant along the line-of-sight and therefore

$$\theta^a = \theta^{a(0)} + \theta^{a(1)} = \theta_o^a - 2 \int_{\eta_s^{(0)}}^{\eta_o} d\eta' \gamma_0^{ab} \partial_b \int_{\eta'}^{\eta_o} d\eta'' \Psi^{(1)}(\eta'', \eta_o - \eta'', \theta_o^a) .$$

Cosmological Observables

To obtain Δ in the PG, in function of the observed redshift and of the direction of observation (θ_o, φ_o) , we have:

Step 1 → Expand the exact expression of Δ in function of the PG coordinate using the coordinate transformation.

Step 2 → Expand conformal time and radial PG coordinates around a fiducial model as $\eta_s = \eta_s^{(0)} + \eta_s^{(1)} + \eta_s^{(2)}$ and $r_s = r_s^{(0)} + r_s^{(1)} + r_s^{(2)}$ perturbatively solving

$$1+z_s = \frac{a(\eta_o)}{a(\eta_s^{(0)})} = \frac{a(\eta_o)}{a(\eta_s)} \left[1 + \delta^{(1)} z + \delta^{(2)} z \right] \quad , \quad w_o = \eta_s^{(0)} + r_s^{(0)} = w^{(0)} + w^{(1)} + w^{(2)}$$

Step 3 → Taylor expand the solution of Step 1 around the fiducial model using Step 2, and around the direction of observation using the fact that $\tilde{\theta}^a = \theta_o^a$ are constant along the line-of-sight and therefore

$$\theta^a = \theta^{a(0)} + \theta^{a(1)} = \theta_o^a - 2 \int_{\eta_s^{(0)}}^{\eta_o} d\eta' \gamma_0^{ab} \partial_b \int_{\eta'}^{\eta_o} d\eta'' \Psi^{(1)}(\eta'', \eta_o - \eta'', \theta_o^a) .$$

Cosmological Observables

To obtain Δ in the PG, in function of the observed redshift and of the direction of observation (θ_o, φ_o) , we have:

Step 1 \rightarrow Expand the exact expression of Δ in function of the PG coordinate using the coordinate transformation.

Step 2 \rightarrow Expand conformal time and radial PG coordinates around a fiducial model as $\eta_s = \eta_s^{(0)} + \eta_s^{(1)} + \eta_s^{(2)}$ and $r_s = r_s^{(0)} + r_s^{(1)} + r_s^{(2)}$ perturbatively solving

$$1+z_s = \frac{a(\eta_o)}{a(\eta_s^{(0)})} = \frac{a(\eta_o)}{a(\eta_s)} \left[1 + \delta^{(1)} z + \delta^{(2)} z \right] \quad , \quad w_o = \eta_s^{(0)} + r_s^{(0)} = w^{(0)} + w^{(1)} + w^{(2)}$$

Step 3 \rightarrow Taylor expand the solution of Step 1 around the fiducial model using Step 2, and around the direction of observation using the fact that $\tilde{\theta}^a = \theta_o^a$ are constant along the line-of-sight and therefore

$$\theta^a = \theta^{a(0)} + \theta^{a(1)} = \theta_o^a - 2 \int_{\eta_s^{(0)}}^{\eta_o} d\eta' \gamma_0^{ab} \partial_b \int_{\eta'}^{\eta_o} d\eta'' \Psi^{(1)}(\eta'', \eta_o - \eta'', \theta_o^a) .$$

Galaxy Number Counts

The (second-order, non-homogeneous, non-averaged) expression of Δ in our perturbed background is so given (in a concise form) by

$$\Delta = \Delta^{(1)}(\mathbf{n}, z_s) + \Delta^{(2)}(\mathbf{n}, z_s)$$

To first order we have (Yoo, Fitzpatrick, Zaldarriaga (2009), Yoo (2010), Bonvin, Durrer (2011), Challinor, Lewis (2011))

$$\begin{aligned} \Delta^{(1)}(\mathbf{n}, z) = & \left(\frac{2}{\mathcal{H}r(z)} + \frac{\mathcal{H}'}{\mathcal{H}^2} \right) \left(\partial_r v^{(1)} + \Psi^{(1)} + 2 \int_0^{r(z)} dr \partial_\eta \Psi^{(1)} \right) - \Psi^{(1)} \\ & + 4\Psi_1 - 2\kappa + \frac{1}{\mathcal{H}} \left(\partial_\eta \Psi^{(1)} + \partial_r^2 v^{(1)} \right) + \delta^{(1)} \end{aligned}$$

with

$$\Psi_1(\mathbf{n}, z) = \frac{2}{r(z)} \int_0^{r(z)} dr \Psi^{(1)}(r) \quad , \quad 2\kappa = -\Delta_2 \psi = 2 \int_0^{r(z)} dr \frac{r(z) - r}{r(z)r} \Delta_2 \Psi^{(1)}(r)$$

Galaxy Number Counts

Keeping only the leading (potentially observables) terms the number counts to second order turns to be

$$\Delta^{(2)} = \Sigma^{(2)} - \langle \Sigma^{(2)} \rangle$$

where

$$\begin{aligned} \Sigma^{(2)}(\mathbf{n}, z) = & \delta^{(2)} + \mathcal{H}^{-1} \partial_r^2 v^{(2)} - 2\kappa^{(2)} + \mathcal{H}^{-2} \left(\partial_r^2 v \right)^2 + \mathcal{H}^{-2} \partial_r v \partial_r^3 v \\ & + \mathcal{H}^{-1} \left(\partial_r v \partial_r \delta + \partial_r^2 v \delta \right) - 2\delta \kappa + \nabla_a \delta \nabla^a \psi \\ & + \mathcal{H}^{-1} \left[-2(\partial_r^2 v) \kappa + \nabla_a (\partial_r^2 v) \nabla^a \psi \right] + 2\kappa^2 - 2\nabla_b \kappa \nabla^b \psi \\ & - \frac{1}{2r(z)} \int_0^{r(z)} dr \frac{r(z) - r}{r} \Delta_2 \left(\nabla^b \psi_1 \nabla_b \psi_1 \right) - 2 \int_0^{r(z)} \frac{dr}{r} \nabla^a \psi_1 \nabla_a \kappa. \end{aligned}$$

with

$$\kappa^{(2)} = \frac{1}{2} \int_0^{r(z)} dr \frac{r(z) - r}{r(z)r} \Delta_2(\Psi + \Phi)^{(2)}(-r\mathbf{n}, \eta_0 - r).$$

Outline

- Introduction
- Geodesic light-cone (GLC) coordinates and cosmological observables
- From GLC to the Poisson gauge: describing the middle non-linear regime
- Galaxy Number Counts: impact of the magnification bias to second order
- Galaxy Number Counts bispectrum
- Conclusions

Magnification Bias

In practice, we cannot observe all galaxies, but only those with a flux which is larger than a certain limit \bar{F} .

If the fluctuation of the source number density N depends on luminosity we have to further Taylor expand to obtain $\Delta(\mathbf{n}, \mathbf{z}, \mathbf{L})$.

This physical threshold impact only the part of the number counts that comes from the galaxy density ρ .

We then obtain (see also Bertacca (2014))

$$\begin{aligned} N(\mathbf{n}, z, \bar{F}) &= N(\mathbf{n}, z) + \frac{\partial}{\partial L} N(\mathbf{n}, z, \bar{L}) (\delta L^{(1)} + \delta L^{(2)}) + \frac{1}{2} \frac{\partial^2}{\partial L^2} N(\mathbf{n}, z, \bar{L}) (\delta L^{(1)})^2 \\ &= N(\bar{z}, \bar{L}) \left[1 + \Delta^{(1)} + \Delta^{(2)} + \frac{\partial_L \bar{\rho}}{\bar{\rho}} (\delta L^{(1)} + \delta L^{(2)}) + \frac{1}{2} \frac{\partial_L^2 \bar{\rho}}{\bar{\rho}} (\delta L^{(1)})^2 \right. \\ &\quad \left. + \frac{(\partial_L \rho - \partial_L \bar{\rho})^{(1)}}{\bar{\rho}} \delta L^{(1)} + \frac{\partial_\eta (\partial_L \bar{\rho})}{\bar{\rho}} \delta L^{(1)} \frac{\delta z^{(1)}}{\mathcal{H}} \right], \end{aligned}$$

On the other hand, $F = L/(2\pi d_L^2)$ and at fixed flux $\delta L = \delta(d_L^2)$.

Magnification Bias

In practice, we cannot observe all galaxies, but only those with a flux which is larger than a certain limit \bar{F} .

If the fluctuation of the source number density N depends on luminosity we have to further Taylor expand to obtain $\Delta(\mathbf{n}, \mathbf{z}, \mathbf{L})$.

This physical threshold impact only the part of the number counts that comes from the galaxy density ρ .

We then obtain (see also Bertacca (2014))

$$\begin{aligned} N(\mathbf{n}, z, \bar{F}) &= N(\mathbf{n}, z) + \frac{\partial}{\partial L} N(\mathbf{n}, z, \bar{L}) (\delta L^{(1)} + \delta L^{(2)}) + \frac{1}{2} \frac{\partial^2}{\partial L^2} N(\mathbf{n}, z, \bar{L}) (\delta L^{(1)})^2 \\ &= N(\bar{z}, \bar{L}) \left[1 + \Delta^{(1)} + \Delta^{(2)} + \frac{\partial_L \bar{\rho}}{\bar{\rho}} (\delta L^{(1)} + \delta L^{(2)}) + \frac{1}{2} \frac{\partial_L^2 \bar{\rho}}{\bar{\rho}} (\delta L^{(1)})^2 \right. \\ &\quad \left. + \frac{(\partial_L \rho - \partial_L \bar{\rho})^{(1)}}{\bar{\rho}} \delta L^{(1)} + \frac{\partial_n (\partial_L \bar{\rho})}{\bar{\rho}} \delta L^{(1)} \frac{\delta z^{(1)}}{\mathcal{H}} \right], \end{aligned}$$

On the other hand, $F = L/(2\pi d_L^2)$ and at fixed flux $\delta L = \delta(d_L^2)$.

Magnification Bias

Defining

$$\left(\frac{\partial \ln \bar{\rho}}{\partial \ln L}\right)(z, \bar{L}) = -\frac{5}{2}s(z, \bar{L}) \quad , \quad \frac{\partial^2}{\partial (\ln L)^2} (\ln \bar{\rho})(z, \bar{L}) = -\frac{5}{2}t(z, \bar{L})$$

$$(1 + \delta^{(1)}) \frac{\partial \ln \rho}{\partial \ln L} - \frac{\partial \ln \bar{\rho}}{\partial \ln L} = -\frac{5}{2}(\delta s)^{(1)}(z, \bar{L})$$

We have, to first order (Challinor, Lewis (2011))

$$\begin{aligned} \Delta^{(1)}(\mathbf{n}, z) = & \left(\frac{2-5s}{\mathcal{H}r(z)} + 5s + \frac{\mathcal{H}'}{\mathcal{H}^2} \right) \left(\partial_r v^{(1)} + \psi^{(1)} + 2 \int_0^{r(z)} dr \partial_\eta \psi^{(1)} \right) \\ & + (5s-1)\psi^{(1)} + (2-5s) \left(2\psi_1 - \kappa^{(1)} \right) \\ & + \frac{1}{\mathcal{H}} \left(\partial_\eta \psi^{(1)} + \partial_r^2 v^{(1)} \right) + \delta^{(1)} \end{aligned}$$

Magnification Bias

While, the leading second order contribution becomes:

$$\begin{aligned}\Sigma^{(2)}(\mathbf{n}, z) = & \delta^{(2)} + \mathcal{H}^{-1} \partial_r^2 v^{(2)} - 2 \left(1 - \frac{5}{2}s\right) \kappa^{(2)} + \mathcal{H}^{-2} \left[\left(\partial_r^2 v\right)^2 + \partial_r v \partial_r^3 v \right] \\ & + \mathcal{H}^{-1} \left(\partial_r v \partial_r \delta + \partial_r^2 v \delta \right) - 2\delta\kappa + \nabla_a \delta \nabla^a \psi \\ & + \mathcal{H}^{-1} \left[-2 \left(1 - \frac{5}{2}s\right) \partial_r^2 v \kappa + \nabla_a \partial_r^2 v \nabla^a \psi \right] + 2 \left(1 - 5s + \frac{25}{4}s^2 - \frac{5}{2}t\right) \kappa^2 \\ & - 2 \left(1 - \frac{5}{2}s\right) \nabla_b \kappa \nabla^b \psi - \left(1 - \frac{5}{2}s\right) \frac{1}{2r(z)} \int_0^{r(z)} dr \frac{r(z) - r}{r} \Delta_2 \left(\nabla^b \psi_1 \nabla_b \psi_1 \right) \\ & - 2 \left(1 - \frac{5}{2}s\right) \int_0^{r(z)} \frac{dr}{r^2} \nabla^a \psi_1 \nabla_a \kappa + 5 (\delta s)^{(1)} \kappa\end{aligned}$$

If the number of galaxies depend on luminosity like a simple power law, $\rho \propto L^p$, we have $s = -2p/5$, $t = 0$ and $(\delta s)^{(1)} = s\delta^{(1)} = -2p\delta^{(1)}/5$.

For $p = -1$ we have $s = 2/5$, $t = 0$ and $(\delta s)^{(1)} = 2\delta^{(1)}/5$

\Downarrow

The pure lensing disappear at first and second order, while the terms $\nabla_a \delta \nabla^a \psi + \mathcal{H}^{-1} \nabla_a \partial_r^2 v \nabla^a \psi$ are not affected by magnification bias.

Outline

- Introduction
- Geodesic light-cone (GLC) coordinates and cosmological observables
- From GLC to the Poisson gauge: describing the middle non-linear regime
- Galaxy Number Counts: impact of the magnification bias to second order
- Galaxy Number Counts bispectrum
- Conclusions

Reduced bispectrum number counts

We define the bispectrum in real space as

$$B(\mathbf{n}_1, \mathbf{n}_2, \mathbf{n}_3, z_1, z_2, z_3) = \langle \Delta(\mathbf{n}_1, z_1) \Delta(\mathbf{n}_2, z_2) \Delta(\mathbf{n}_3, z_3) \rangle_c$$

Expanding the direction dependence of Δ in spherical harmonics

$$B(\mathbf{n}_1, \mathbf{n}_2, \mathbf{n}_3, z_1, z_2, z_3) = \sum_{\ell_i, m_i} B_{\ell_1 \ell_2 \ell_3}^{m_1 m_2 m_3}(z_1, z_2, z_3) Y_{\ell_1 m_1}(\mathbf{n}_1) Y_{\ell_2 m_2}(\mathbf{n}_2) Y_{\ell_3 m_3}(\mathbf{n}_3)$$

and

$$B_{\ell_1 \ell_2 \ell_3}^{m_1 m_2 m_3}(z_1, z_2, z_3) = \mathcal{G}_{\ell_1, \ell_2, \ell_3}^{m_1, m_2, m_3} b_{\ell_1, \ell_2, \ell_3}(z_1, z_2, z_3)$$

with

$$\mathcal{G}_{\ell_1, \ell_2, \ell_3}^{m_1, m_2, m_3} \\ b_{\ell_1, \ell_2, \ell_3}(z_1, z_2, z_3)$$

Gaunt integral

Reduced bispectrum

Reduced bispectrum number counts

Assuming Gaussian initial condition

$$\langle \Delta^{(1)}(\mathbf{n}_1, z_1) \Delta^{(1)}(\mathbf{n}_2, z_2) \Delta^{(1)}(\mathbf{n}_3, z_3) \rangle_c = 0$$

we compute the contribution coming from

$$\langle \Delta^{(2)}(\mathbf{n}_1, z_1) \Delta^{(1)}(\mathbf{n}_2, z_2) \Delta^{(1)}(\mathbf{n}_3, z_3) \rangle_c + \text{permutations}$$

taking only the second order leading terms and $\Delta^{(1)} = \delta^{(1)}$.

We then divide our leading reduced bispectrum as follow

$$\begin{aligned} b_{\ell_1 \ell_2 \ell_3} = & \textcolor{blue}{b_{\ell_1 \ell_2 \ell_3}^{\delta^{(2)}}} + \textcolor{blue}{b_{\ell_1 \ell_2 \ell_3}^{\nu^{(2)'}}} + \textcolor{blue}{b_{\ell_1 \ell_2 \ell_3}^{\nu'^2}} + \textcolor{blue}{b_{\ell_1 \ell_2 \ell_3}^{\nu\nu''}} + \textcolor{blue}{b_{\ell_1 \ell_2 \ell_3}^{\nu\delta'}} + \textcolor{blue}{b_{\ell_1 \ell_2 \ell_3}^{\nu'\delta}} \\ & + \textcolor{orange}{b_{\ell_1 \ell_2 \ell_3}^{\kappa^{(2)}}} + \textcolor{orange}{b_{\ell_1 \ell_2 \ell_3}^{\kappa\delta}} + \textcolor{orange}{b_{\ell_1 \ell_2 \ell_3}^{\nabla\delta\nabla\psi}} + \textcolor{orange}{b_{\ell_1 \ell_2 \ell_3}^{\nu'\kappa}} + \textcolor{orange}{b_{\ell_1 \ell_2 \ell_3}^{\nabla\nu'\nabla\psi}} \\ & + \textcolor{green}{b_{\ell_1 \ell_2 \ell_3}^{\kappa^2}} + \textcolor{green}{b_{\ell_1 \ell_2 \ell_3}^{\nabla\kappa\nabla\psi}} + \textcolor{green}{b_{\ell_1 \ell_2 \ell_3}^{\int\nabla\kappa\nabla\Psi_1}} + \textcolor{green}{b_{\ell_1 \ell_2 \ell_3}^{\int\Delta_2(\nabla\Psi_1\nabla\Psi_1)}} \end{aligned}$$

where the color coding indicates

Newtonian terms

Newtonian x lensing terms

Lensing terms

Reduced bispectrum number counts: a simple example

Let us consider the monopole term of the second order density

$$\delta^{(2)0}(\mathbf{k}_1, \eta) = \frac{17}{21} \frac{1}{(2\pi)^3} \int d^3k \delta^{(1)}(\mathbf{k}, \eta) \delta^{(1)}(\mathbf{k}_1 - \mathbf{k}, \eta).$$

We introduce the initial curvature power spectrum from linear perturbation theory by

$$\langle R_{\text{in}}(\mathbf{k}) R_{\text{in}}(\mathbf{k}') \rangle = (2\pi)^3 \delta_D(\mathbf{k} + \mathbf{k}') P_R(k).$$

The transfer function $T_A(\eta, k)$ of a given variable A by

$$A(\eta, \mathbf{k}) = T_A(\eta, k) R_{\text{in}}(\mathbf{k}),$$

and the angular power spectra by

$$\langle A(z_1, \vec{\ell}), \bar{B}(z_2, \vec{\ell}') \rangle = \delta_D(\vec{\ell} - \vec{\ell}') c_\ell^{AB}(z_1, z_2)$$

$$c_\ell^{AB}(z_1, z_2) = \frac{2}{\pi} \int dk k^2 P_R(k) \Delta_\ell^A(z_1, k) \Delta_\ell^B(z_2, k),$$

with $\Delta_\ell^A(z, k)$ the transfer function in angular and redshift space for the variable A .

Reduced bispectrum number counts: a simple example

We first obtain

$$\begin{aligned} & \langle \delta^{(2)0}(\mathbf{n}_1, z_1) \delta^{(1)}(\mathbf{n}_2, z_2) \delta^{(1)}(\mathbf{n}_3, z_3) \rangle_c \\ &= \frac{17}{21} \frac{2}{(2\pi)^6} \int d^3 k_2 d^3 k_3 P(k_2) P(k_3) T_\delta(k_2, \eta_1) T_\delta(k_3, \eta_1) \\ & \quad \times T_\delta(k_2, \eta_2) T_\delta(k_3, \eta_3) e^{-i(\mathbf{k}_2 \cdot \mathbf{n}_1 r_1 + \mathbf{k}_3 \cdot \mathbf{n}_1 r_1)} e^{i(\mathbf{k}_2 \cdot \mathbf{n}_2 r_2 + \mathbf{k}_3 \cdot \mathbf{n}_3 r_3)} . \end{aligned}$$

Then, expanding the Fourier modes in spherical harmonics and Bessel functions

$$e^{i\mathbf{k} \cdot \mathbf{n}r} = 4\pi \sum_{\ell m} i^\ell j_\ell(kr) Y_{\ell m}(\mathbf{n}) Y_{\ell m}^*(\hat{\mathbf{k}}) ,$$

we can finally find

$$b_{\ell_1 \ell_2 \ell_3}^{\delta 0} = \frac{34}{21} \left[c_{\ell_2}^{\delta\delta}(z_1, z_2) c_{\ell_3}^{\delta\delta}(z_1, z_3) + c_{\ell_1}^{\delta\delta}(z_1, z_2) c_{\ell_3}^{\delta\delta}(z_2, z_3) + c_{\ell_1}^{\delta\delta}(z_1, z_3) c_{\ell_2}^{\delta\delta}(z_2, z_3) \right]$$

where we have used

$$\Delta_\ell^\delta(z, k) = T_\delta(\eta(z), k) j_\ell(kr(z)) ,$$

for the first order density.

Reduced bispectrum number counts

More in general, we can express all the reduced bispectra in terms of products of angular power spectra, except for the second order terms $\delta^{(2)}$, $v^{(2)}$ and $\kappa^{(2)}$.

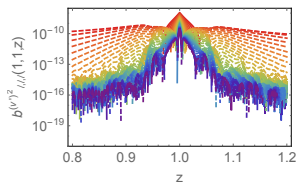
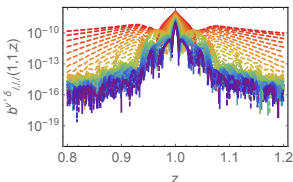
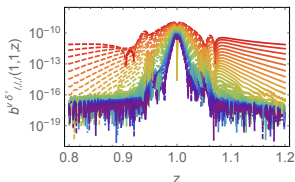
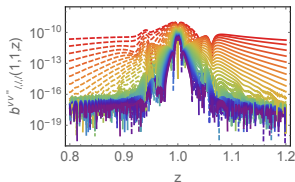
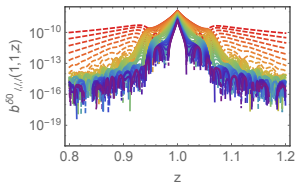
For instance, most of our contributions are of the form

$$\begin{aligned} b_{\ell_1 \ell_2 \ell_3}^{p_\alpha p_\beta}(z_1, z_2, z_3) \sim & c_{\ell_2}^{p_\alpha \delta}(z_1, z_2) c_{\ell_3}^{p_\beta \delta}(z_1, z_3) + c_{\ell_3}^{p_\alpha \delta}(z_1, z_3) c_{\ell_2}^{p_\beta \delta}(z_1, z_2) \\ & + c_{\ell_1}^{p_\alpha \delta}(z_2, z_1) c_{\ell_3}^{p_\beta \delta}(z_2, z_3) + c_{\ell_3}^{p_\alpha \delta}(z_2, z_3) c_{\ell_1}^{p_\beta \delta}(z_2, z_1) \\ & + c_{\ell_1}^{p_\alpha \delta}(z_3, z_1) c_{\ell_2}^{p_\beta \delta}(z_3, z_2) + c_{\ell_2}^{p_\alpha \delta}(z_3, z_2) c_{\ell_1}^{p_\beta \delta}(z_3, z_1), \end{aligned}$$

where p_α and p_β denote any perturbation.

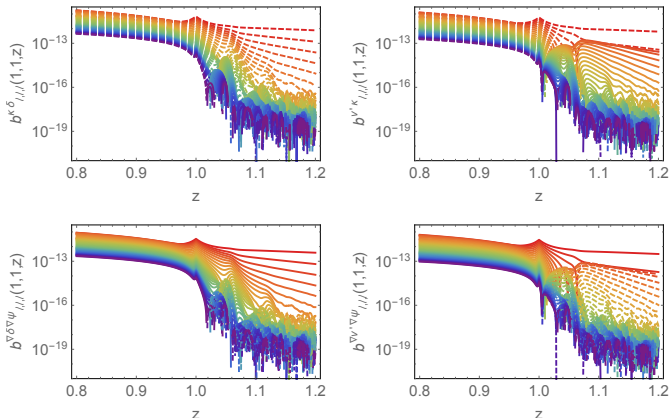
We plot their numerical results in the following slides.

Newtonian terms



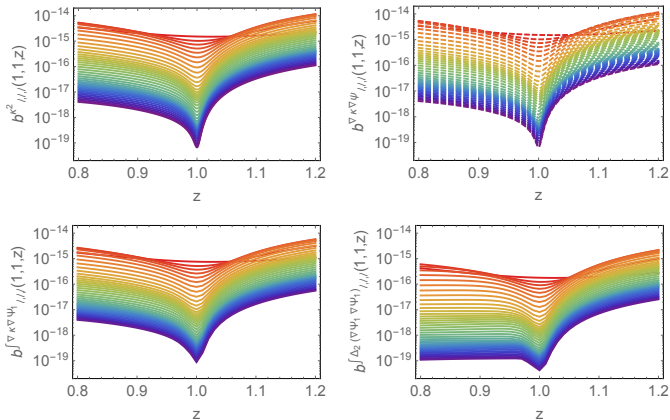
We plot the contributions from the Newtonian terms to the bispectrum for different values of $\ell = \ell_1 = \ell_2 = \ell_3$, from $\ell = 4$ (red) to $\ell = 400$ (purple), as a function of the third redshift $z_3 = z$ for $z_1 = z_2 = 1$.

Newtonian x lensing terms



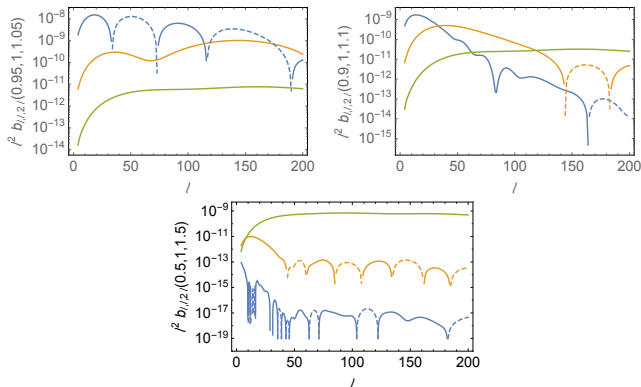
We plot the contributions from the Newtonian \times lensing terms to the bispectrum for different values of $\ell = \ell_1 = \ell_2 = \ell_3$, from $\ell = 4$ (red) to $\ell = 400$ (purple), as a function of the third redshift $z_3 = z$ for $z_1 = z_2 = 1$.

Lensing terms



We plot the contributions from the pure lensing terms to the bispectrum for different values of $\ell = \ell_1 = \ell_2 = \ell_3$, from $\ell = 4$ (red) to $\ell = 400$ (purple), as a function of the third redshift $z_3 = z$ for $z_1 = z_2 = 1$.

Reduced bispectrum number counts: redshift separation

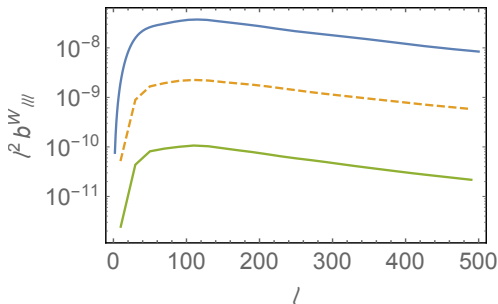


We plot the contributions from the Newtonian terms (blue), the Newtonian \times lensing terms (yellow) and the pure lensing terms (green) for $z_1 = 0.95$, $z_2 = 1$ and $z_3 = 1.05$ (top left), for $z_1 = 0.9$, $z_2 = 1$ and $z_3 = 1.1$ (top right) and for $z_1 = 0.5$, $z_2 = 1$ and $z_3 = 1.5$ (bottom) as function of $\ell = \ell_1 = \ell_2 = \ell_3/2$. Dashed lines correspond to negative values.

Reduced bispectrum number counts: redshift bin

Observed reduced bispectrum:

$$b_{\ell_1 \ell_2 \ell_3}^W(z_1, z_2, z_3) = \int dz'_1 dz'_2 dz'_3 b_{\ell_1 \ell_2 \ell_3}(z'_1, z'_2, z'_3) W(z_1, z'_1) W(z_2, z'_2) W(z_3, z'_3)$$



We plot the contributions to the bispectrum with window function of width $\Delta z = 1$ and mean redshift $z = 1$, for Newtonian (blue), Lensing \times Newtonian (yellow) and Lensing (green). Dashed lines correspond to negative values.

Conclusions

- We have presented the geodesic light-cone coordinates, a coordinate system adapted to an observer and his past light-cone.
- In the framework of the GLC we can write LSS observables in an exact, non-perturbative way.
- We have show the leading perturbative expressions for the number counts at second order as a function of the observed redshift and the direction of the observation.
- We have defined the number counts reduced bispectrum in the directly observable spherical-harmonics-redshift space.
- In particular configurations the integrated relativistic terms can dominate the signal/be not negligible
 - Well separated redshifts.
 - Broad window functions.

Outlook: Evaluation of the signal-to-noise to investigate whether planned surveys can detect the lensing signal when it dominates.

Conclusions

- We have presented the geodesic light-cone coordinates, a coordinate system adapted to an observer and his past light-cone.
- In the framework of the GLC we can write LSS observables in an exact, non-perturbative way.
- We have show the leading perturbative expressions for the number counts at second order as a function of the observed redshift and the direction of the observation.
- We have defined the number counts reduced bispectrum in the directly observable spherical-harmonics-redshift space.
- In particular configurations the integrated relativistic terms can dominate the signal/be not negligible
 - Well separated redshifts.
 - Broad window functions.

Outlook: Evaluation of the signal-to-noise to investigate whether planned surveys can detect the lensing signal when it dominates.

Conclusions

- We have presented the geodesic light-cone coordinates, a coordinate system adapted to an observer and his past light-cone.
- In the framework of the GLC we can write LSS observables in an exact, non-perturbative way.
- We have show the leading perturbative expressions for the number counts at second order as a function of the observed redshift and the direction of the observation.
- We have defined the number counts reduced bispectrum in the directly observable spherical-harmonics-redshift space.
- In particular configurations the integrated relativistic terms can dominate the signal/be not negligible
 - Well separated redshifts.
 - Broad window functions.

Outlook: Evaluation of the signal-to-noise to investigate whether planed surveys can detect the lensing signal when it dominates.

Conclusions

- We have presented the geodesic light-cone coordinates, a coordinate system adapted to an observer and his past light-cone.
- In the framework of the GLC we can write LSS observables in an exact, non-perturbative way.
- We have show the leading perturbative expressions for the number counts at second order as a function of the observed redshift and the direction of the observation.
- We have defined the number counts reduced bispectrum in the directly observable spherical-harmonics-redshift space.
- In particular configurations the integrated relativistic terms can dominate the signal/be not negligible
 - Well separated redshifts.
 - Broad window functions.

Outlook: Evaluation of the signal-to-noise to investigate whether planed surveys can detect the lensing signal when it dominates.

Conclusions

- We have presented the geodesic light-cone coordinates, a coordinate system adapted to an observer and his past light-cone.
- In the framework of the GLC we can write LSS observables in an exact, non-perturbative way.
- We have show the leading perturbative expressions for the number counts at second order as a function of the observed redshift and the direction of the observation.
- We have defined the number counts reduced bispectrum in the directly observable spherical-harmonics-redshift space.
- In particular configurations the integrated relativistic terms can dominate the signal/be not negligible
 - Well separated redshifts.
 - Broad window functions.

Outlook: Evaluation of the signal-to-noise to investigate whether planed surveys can detect the lensing signal when it dominates.

Conclusions

- We have presented the geodesic light-cone coordinates, a coordinate system adapted to an observer and his past light-cone.
- In the framework of the GLC we can write LSS observables in an exact, non-perturbative way.
- We have show the leading perturbative expressions for the number counts at second order as a function of the observed redshift and the direction of the observation.
- We have defined the number counts reduced bispectrum in the directly observable spherical-harmonics-redshift space.
- In particular configurations the integrated relativistic terms can dominate the signal/be not negligible
 - Well separated redshifts.
 - Broad window functions.

Outlook: Evaluation of the signal-to-noise to investigate whether planned surveys can detect the lensing signal when it dominates.

Conclusions

- We have presented the geodesic light-cone coordinates, a coordinate system adapted to an observer and his past light-cone.
- In the framework of the GLC we can write LSS observables in an exact, non-perturbative way.
- We have show the leading perturbative expressions for the number counts at second order as a function of the observed redshift and the direction of the observation.
- We have defined the number counts reduced bispectrum in the directly observable spherical-harmonics-redshift space.
- In particular configurations the integrated relativistic terms can dominate the signal/be not negligible
 - Well separated redshifts.
 - Broad window functions.

Outlook: Evaluation of the signal-to-noise to investigate whether planned surveys can detect the lensing signal when it dominates.

THANKS FOR THE ATTENTION!

Coordinates Trasformation

Let us introduce the following auxiliary quantities:

$$P(\eta, r, \theta^a) = \int_{\eta_{in}}^{\eta} d\eta' \frac{a(\eta')}{a(\eta)} \Psi(\eta', r, \theta^a) \quad , \quad Q(\eta_+, \eta_-, \theta^a) = \int_{\eta_o}^{\eta_-} dx \hat{\Psi}(\eta_+, x, \theta^a) \quad ,$$

where $\eta_{\pm} = \eta \pm r$. We then obtain

$$\begin{aligned} \tau &= \tau^{(0)} + \tau^{(1)} + \tau^{(2)} \\ &\equiv \left(\int_{\eta_{in}}^{\eta} d\eta' a(\eta') \right) + a(\eta)P + \int_{\eta_{in}}^{\eta} d\eta' \frac{a(\eta')}{2} \left[\Phi^{(2)} - \Psi^2 + (\partial_r P)^2 + \gamma_0^{ab} \partial_a P \partial_b P \right] (\eta', r, \theta^a) \\ w &= w^{(0)} + w^{(1)} + w^{(2)} \\ &\equiv \eta_+ + Q + \frac{1}{4} \int_{\eta_o}^{\eta_-} dx \left[\hat{\Psi}^{(2)} + \hat{\Phi}^{(2)} + 4\hat{\Psi} \partial_+ Q + \hat{\gamma}_0^{ab} \partial_a Q \partial_b Q \right] (\eta_+, x, \theta^a) \\ \tilde{\theta}^a &= \tilde{\theta}^{a(0)} + \tilde{\theta}^{a(1)} + \tilde{\theta}^{a(2)} \equiv \theta^a + \frac{1}{2} \int_{\eta_o}^{\eta_-} dx \left[\hat{\gamma}_0^{ab} \partial_b Q \right] (\eta_+, x, \theta^a) + \int_{\eta_o}^{\eta_-} dx \left[\frac{1}{2} \gamma_o^{ac} \partial_c w^{(2)} \right. \\ &\quad \left. + \hat{\Psi} \left(\gamma_o^{ac} \partial_c w^{(1)} + \partial_+ \tilde{\theta}^{a(1)} \right) - \partial_+ w^{(1)} \partial_- \tilde{\theta}^{a(1)} + \frac{1}{2} \gamma_o^{dc} \partial_d w^{(1)} \partial_c \tilde{\theta}^{a(1)} \right] (\eta_+, x, \theta^a) \end{aligned}$$

Coordinates Trasformation

The non-trivial entries of the GLC metric are then given by

$$\Upsilon^{-1} = \frac{1}{a(\eta)} \left(1 + \partial_+ Q - \partial_r P + \partial_\eta w^{(2)} + \frac{1}{a} (\partial_\eta - \partial_r) \tau^{(2)} - \Psi \partial_\eta Q - \Phi^{(2)} \right. \\ \left. + 2\Psi^2 - \partial_r P \partial_r Q - 2\Psi \partial_r P - \gamma_0^{ab} \partial_a P \partial_b Q \right)$$

$$U^a = \partial_\eta \tilde{\theta}^{a(1)} - \frac{1}{a} \gamma_0^{ab} \partial_b \tau^{(1)} + \partial_\eta \tilde{\theta}^{a(2)} - \frac{1}{a} \gamma_0^{ab} \partial_b \tau^{(2)} - \frac{1}{a} \partial_r \tau^{(1)} \partial_r \tilde{\theta}^{a(1)} - \Psi \left(\partial_\eta \tilde{\theta}^{a(1)} \right. \\ \left. + \frac{2}{a} \gamma_0^{ab} \partial_b \tau^{(1)} \right) - \frac{1}{a} \gamma_0^{cd} \partial_c \tau^{(1)} \partial_d \tilde{\theta}^{a(1)} + (\partial_+ Q - \partial_r P) \left(-\partial_\eta \tilde{\theta}^{a(1)} + \frac{1}{a} \gamma_0^{ab} \partial_b \tau^{(1)} \right) ,$$

$$a(\eta)^2 \gamma^{ab} = \gamma_0^{ab} (1 + 2\Psi) + \left[\gamma_0^{ac} \partial_c \tilde{\theta}^{b(1)} + (a \leftrightarrow b) \right] + \gamma_0^{ab} \left(\Psi^{(2)} + 4\Psi^2 \right) - \partial_\eta \tilde{\theta}^{a(1)} \partial_\eta \tilde{\theta}^{b(1)} \\ + \partial_r \tilde{\theta}^{a(1)} \partial_r \tilde{\theta}^{b(1)} + 2\Psi \left[\gamma_0^{ac} \partial_c \tilde{\theta}^{b(1)} + (a \leftrightarrow b) \right] + \gamma_0^{cd} \partial_c \tilde{\theta}^{a(1)} \partial_d \tilde{\theta}^{b(1)} \\ + \left[\gamma_0^{ac} \partial_c \tilde{\theta}^{b(2)} + (a \leftrightarrow b) \right] .$$